An intercomparison between the surface heat flux feedback in five coupled models, COADS and the NCEP reanalysis

C. Frankignoul[1], E. Kestenare[1], M. Botzet[2], A. F. Carril[3], H. Drange[4], A. Pardaens[5], L. Terray[6] and R. Sutton[7]

(1) Université Pierre et Marie Curie, Institute Pierre-Simon Laplace, Laboratoire d' Océanographie Dynamique et de Climatologie, 4 place Jussieu, 75252 Paris Cedex 05, France,

(2) Max-Planck-Institut für Meteorologie, Hamburg, Germany,

(3) Istituto Nazionale di Geofisica e Vulcanologia, Bologna, Italy,

(4) Nansen Environmental and Remote Sensing Center, Bergen, Norway,

(5) Hadley Centre for Climate Prediction and Research, Met Office, UK,

(6) CERFACS, Toulouse, France,

(7) Department of Meteorology, University of Reading, UK,

Abstract

The surface heat flux feedback is estimated in the Atlantic and the extra-tropical Indo-Pacific, using monthly heat flux and sea surface temperature anomaly data from control simulations with five global climate models, and it is compared to estimates derived from COADS and the NCEP reanalysis. In all data sets, the heat flux feedback is negative nearly everywhere and damps the sea surface temperature anomalies. At extra-tropical latitudes, it is strongly dominated by the turbulent fluxes. The radiative feedback can be positive or negative, depending on location and season, but it remains small, except in some models in the tropical Atlantic. The negative heat flux feedback is strong in the mid-latitude storm tracks, exceeding 40 W m^{-2} K^{-1} at place, but in the Northern Hemisphere it is substantially underestimated in several models. The negative feedback weakens at high latitudes, although the models do not reproduce the weak positive feedback found in NCEP in the northern North Atlantic. The main differences are found in the tropical Atlantic where the heat flux feedback is weakly negative in some models , as in the observations, and strongly negative in others where it can exceed 30 W m^{-2} K^{-1} at large scales, in part because of a strong contribution of the radiative fluxes, in particular during spring. A comparison between models with similar atmospheric or oceanic components suggests that the atmospheric model is primarily responsible for the heat flux feedback differences at extra-tropical latitudes. In the tropical Atlantic, the ocean behavior plays an equal role. The differences in heat flux feedback in the tropical Atlantic are reflected in the sea surface temperature anomaly persistence, which is too small in models where the heat flux damping is large. A good representation of the heat flux feedback is thus required to simulate climate variability realistically.

1 Introduction

The surface heat flux plays a dual role in the dynamics of large-scale sea surface temperature (SST) anomalies: it largely contributes to their generation, but it also affects their evolution after they have been generated, thereby acting as a feedback (Frankignoul and Hasselmann *1977*). The heat flux feedback thus controls in part the persistence and the amplitude of the

SST anomalies. As it also determines the flux of energy exchanged with the atmosphere that is associated with a SST anomaly of given amplitude, it plays an important role at low frequency and must be well represented in climate models.

As shown by Frankignoul et al. (*1998*, hereafter FCL), the heat flux feedback can be estimated at extra-tropical latitudes from the observations. Because of the short time scale of the intrinsic variability of the atmosphere, the covariance between atmospheric and SST anomalies is negligible when SST leads by more than the atmospheric persistence if the SST anomalies have no influence on the atmosphere. If they have an influence, then the covariance does not vanish but decays with increasing lead time as the SST anomalies. FCL used this property to show that the turbulent (latent and sensible) heat flux feedback derived from the COADS observations was always negative in the central and eastern North Atlantic, thereby damping the SST anomalies. It averaged about 20 W m^{-2} K^{-1}, and was stronger during fall and winter than during summer. The analysis was extended by Frankignoul and Kestenare (*2002*, hereafter FK) to the Atlantic and the North Pacific, using both COADS and the NCEP reanalysis. At extra tropical latitudes, the heat flux feedback was shown to be negative and dominated by the turbulent fluxes, mostly ranging between 10 and 40 W m^{-2} K^{-1}. Depending on season and location, the radiative feedback could be positive or negative, but it was generally small.

In the tropics, the statistical signature of the air-sea interactions is more difficult to interpret as the ocean–atmosphere coupling is stronger. In the tropical Pacific, the coupling is so strong that the oceanic and atmospheric fluctuations mostly have the same time scale, so that FCL's method cannot be used. Nonetheless, the observations suggest that the heat flux feedback is negative in the equatorial Pacific (Ramanathan and Collins *1991*). In the tropical Atlantic, the coupling is weaker and the atmospheric fluctuations less persistent. FCL's method can be thus be used, at least if the influence of the El Niño – Southern Oscillation (ENSO) in the tropical Pacific can be removed (the ENSO teleconnections bias the heat flux feedback estimates toward positive feedback, sustained atmospheric forcing being interpreted as an atmospheric response to the SST anomalies). FK found that the heat flux feedback was weak but negative (consistent with Czaja et al. *2002*). The wind-evaporation-SST (WES) feedback (Xie and Philander *1994*; Chang et al. *1997*) is thus not strong enough to sustain the SST anomaly "dipole" (although the SST anomalies are largely uncorrelated between either side of the equator), contrary to what had been suggested by Chang et al. (*1997*; *2001*) based on an analysis where the ENSO forcing had not been removed.

As reviewed by Frankignoul et al. (*1998*) and FK, estimates of the heat flux feedback have been derived from the response of atmospheric general circulation models (GCMs) to prescribed SST anomalies. However, the results of these sensitivity studies may not apply to a more realistic setting where the SST anomalies are allowed to vary. Indeed, as the SST anomalies primarily result from the natural variability of the atmosphere, the feedback should be weaker at low frequency where the SST has time to adjust to the air temperature fluctuations, reducing the air–sea contrast (Barsugli and Battisti *1998*). Also, if the SST anomalies result from an oceanic heat flux convergence, they may not be co-located with the surface heat flux (Sutton and Mathieu *2002*). In view of this complexity, GCM validation should be done in the coupled mode.

Qualitative estimates have been made in a few coupled models: the mid-latitude heat flux feedback was argued to be positive in the ECHAM3/HOPE coupled model (Latif and Barnett *1994*; Grötzner et al. *1998*), but found to be negative in ECHAM1/LSG (Zorita and

Frankignoul *1997*; Frankignoul et al. *2000*) and ECHAM3/LSG (von Storch *2000*). In Frankignoul et al. (*2002*), the heat flux feedback in the Atlantic was estimated in the ECHAM4/OPA8 model in exactly the same conditions as when using observations, allowing for a more quantitative comparison. The model heat flux feedback was found to be realistic at mid latitudes but much too negative in the tropical Atlantic.

Since the heat flux feedback estimates in FK were generally similar for COADS and NCEP, they may be used for model validation. In this work, the heat flux feedback is estimated in the five climate models (Sect. 2) that have been used in the PREDICATE project of the European Community, and it is compared to the observations. Since the method (Sect. 3) is based on a separation between atmospheric and SST anomaly time scales, it cannot be used in the tropical Pacific where the ocean–atmosphere coupling is very strong. The ENSO influence is strong in the tropical Indian ocean, in particular in the east, and it is thus not considered. The heat flux feedback is estimated in the other ice-free areas, with emphasis on the Atlantic where a detailed comparison is conducted (Sect. 4). The influence of the heat flux feedback on SST anomaly persistence is illustrated in Sect. 5. Discussion and conclusions are given in Sect. 6.

2 The coupled models

Control simulations from the five global coupled ocean–atmosphere GCMs used in PREDICATE are considered. These models typically represent very late 1990s or early 2000s vintage and include sea-ice models that take into account advection. The Bergen Climate Model (BCM) is described in Furevik et al. (*2003*), the CERFACS one in Jouzeau et al. (*2003*), HADCM3 in Gordon et al. (*2000*), and the ECHAM5/MPI-OM1 (MPI) model in Latif et al. (Submitted 2003). The INGV model is the SINTEX model (Guardi et al. *2003*), except that the original relaxation to climatology has been replaced by a coupling with the Louvain La Neuve dynamic sea-ice model (Fichefet and Morales Maqueda *1997*). Table 1 describes some salient features of their atmosphere and ocean, and gives additional references. The Bergen model used fixed "flux adjustment" for heat and freshwater, while the other models were run without flux correction. All coupled models show the usual biases (e.g., Davey et al. *2002*): for instance, the SST is too warm (cold) in the eastern (western) South Atlantic, too cold in the subtropical gyre of the North Atlantic (except near the too northerly path of the Gulf Stream), and too warm in the Southeastern Pacific. In the subpolar gyre, the SST can be too warm (INGV), too cold (CERFACS, Hadley, MPI), or slightly too warm in the west and too cold in the east (BCM). Note that, because of the flux correction, the SST climatology is more realistic in BCM, although the equatorial Atlantic is too cold.

Table 1 Model details and additional references

Model	**Atmosphere**	**Ocean**	**Integration years**
BCM	ARPEGE cycle 15	MICOM	113–233
	T_L 63, L31	0.8–2.4 × 2.4, L24	
	Déqué et al. (*1994*)	Bleck et al. (*1992*)	
CERFACS	ARPEGE-Climat version 3	OPA 8.1	70–200
	T63 (except physics), L31	0.5–2 × 2, L31	
	Déqué et al. (*1994*)	Madec et al. (*1998*)	
HadCM3	HadAM3	HadOM3	541–671

Model	Atmosphere	Ocean	Integration years
	2.5 × 3.75, L19	1.25 × 1.25, L20	
	Pope et al. (*2000*)	Gordon et al. (*2000*)	
INGV	ECHAM4	OPA8.1	1–95
	T42, L19	0.5–2 × 2, L31	
	Roeckner et al. (*1996*)	Madec et al. (*1998*)	
MPI	ECHAM5	MPI-OM1	72–202
	T42, L19	About 0.5–2.8 × 2.8, L23	
	Roeckner et al. (*2003*)	Marsland et al. (*2003*)	

Atmosphere: Tn denotes triangular spectral at wave number *n*, the L-index linear grid, and Ln *n* vertical levels. In CERFACS, diabatic and nonlinear terms are calculated on a T42 gaussian grid. Ocean: latitude x longitude; A–B denotes irregular oceanic resolution ranging between A and B. Integration years are given after spin-up

In all but one case, we used 131 years of integration in approximate statistically steady state. We used monthly anomalies from the mean seasonal cycle of SST, turbulent (latent plus sensible) heat flux, and net (shortwave plus longwave) surface radiation on the atmospheric model grid (the Gaussian grid for spectral models). To reduce the influence of trends and low-frequency changes, a third-order polynomial was removed from the monthly data by least squares fit. Since the estimation of the heat flux feedback requires that the oceanic influence on the atmosphere be weak and the atmospheric spectra essentially white at low frequency, the tropical Indo-Pacific between 20°S and 20°N was not considered. Elsewhere we removed (some of) the ENSO influence by seasonal regression analysis, as described in Sect. 3.

For comparison, we use the feedback that FK similarly estimated using monthly SST and surface heat flux anomalies from the Comprehensive Ocean-Atmosphere Data Set (COADS) for 1950–97 (Atlantic) or 1958–97 (North Pacific) on a 5° × 5° grid. We also recomputed for 1958–2001 the heat flux feedback from the monthly SST and surface heat flux anomalies of the NCEP/NCAR Reanalysis Project (Kalnay et al. *1996*) on their 1.9° × 1.9° grid, with results similar to those obtained by FK for the 1958–98 period, adding for completeness the southern Indo-Pacific between 20 and 40°S; regions further south were not considered because of the lack of reliability of the NCEP reanalysis between 1979 and 1992 (Trenberth et al. *2001*). The differences between COADS and NCEP provide an indication of the uncertainty of the "observational" estimates. However, note that the COADS data were only lightly filtered by FK and remained noisy, and that the NCEP turbulent heat flux is biased high in the North Atlantic, while the shortwave gain tends to be underestimated (see Josey *2001* and references therein). Also, because of sparse data, the heat flux feedback in the Southern Hemisphere is poorly documented in COADS, and less constrained by observations in NCEP.

To prevent the heat flux feedback estimates being contaminated by the presence of sea ice, grid points that had a sea-ice concentration in excess of 20% during at least one winter were excluded from the analysis (this stringent criterion roughly corresponds to a maximum climatological sea-ice concentration of 5%). As shown by the blackened areas in the figures below, the sea-ice extension varies between models. In the Northern Hemisphere, it is realistic

(as compared with NCEP) in INGV, but somewhat larger than observed in CERFACS, HADCM3, and MPI, and smaller in BCM.

3 Estimation of the heat flux feedback

Let us assume that the anomaly Q' in the surface heat flux (positive downward) can be decomposed into

$$Q'(t) = q'(t) - \alpha T'(t) \quad (1)$$

where q' is independent of the SST anomaly T', $-\alpha T'$ is the heat flux anomaly induced by T', and α the heat flux feedback (in W m^{-2} K^{-1}, positive for negative feedback). This assumes that the heat flux adjustment to a SST anomaly is linear and fast so that the atmospheric boundary layer reaches a balance quite rapidly compared to the time rate of change of the SST anomaly. The cross-covariance $R_{TQ}(\tau)$ at lag τ between T' and Q' is then given by

$$R_{TQ}(\tau) = R_{Tq}(\tau) - \alpha R_{TT}(\tau) \quad (2)$$

where R_{Tq} is the cross-covariance between T' and q', and R_{TT} the auto-covariance of T'.

At extra-tropical latitudes, q' represents the part of the heat flux anomalies which is solely controlled by the atmospheric dynamics. As it is well modeled by a short time scale stochastic process, $R_{Tq}(\tau)$ vanishes when T' leads q' by more than the atmospheric persistence. The feedback is thus given at sufficiently large negative lag by

$$\alpha = -R_{TQ}(\tau)/R_{TT}(\tau) \quad (3)$$

which can be estimated from observed or model data. When using monthly anomalies, Eq. (3) holds to a good approximation at all negative lags, although it neglects the small contribution of R_{Tq} that may be associated at lag –1 month with atmospheric persistence. Since Eq. (3) become too noisy at large lags to provide useful information, α will be estimated as in FK by averaging the values of α obtained at lag –1, –2, and –3 (–1 for seasonal estimates) if the persistence of the SST anomalies is sufficiently large for their auto-correlation to differ from zero at the 5% level, assuming independent samples. If no lag qualifies, the feedback is set to zero. In the equatorial Atlantic, q' may become persistent, because of changes in the intrinsic atmospheric variability and stronger ocean–atmosphere coupling. Use of relation (3) then leads to heat flux feedback estimates that are biased toward positive feedback (see FK).

A similar bias results from global ENSO teleconnections that add a persistent component to the heat flux anomalies. Assuming linearity, the heat flux can then be written at each grid point

$$Q'(t) = q'(t) - \alpha T'(t) + \beta N'(t), \quad (4)$$

where $N'(t)$ represents the (slowly varying) ENSO time behavior and β measures the heat flux associated with the ENSO teleconnections. As $R_{TN}(\tau)$ does not vanish at negative lag, Eq. (3) would provide an estimate of the heat flux feedback that is biased toward positive feedback. As shown by FK, unbiased estimates can be obtained, at least within the framework of the simplified model Eq. (4), by removing the ENSO signal by regression analysis from both the heat flux and the SST anomaly data. Thus we define corrected anomalies by

$\tilde{T}(t) = T(t) - \delta N'(t)$ and $\tilde{Q}'(t) = Q'(t) - \gamma N'(t) \approx q'(t) - \alpha \tilde{T}(t)$, where δ and γ are calculated by least squares fit, and γ is an estimate of $\beta - \alpha\delta$. One then has,

$$R_{\tilde{T}\tilde{Q}}(\tau) \approx R_{\tilde{T}q}(\tau) - \alpha R_{\tilde{T}\tilde{T}}(\tau) \quad (5)$$

so that Eq. (3) remains applicable at negative lags for corrected variables. Note that Eq. (4) neglects the observed non-linearity of the ENSO teleconnections, (Hoerling et al. *1997*), but easily allows for seasonal dependence. Following FK, ENSO was defined in each data set by the first two principal components of the monthly SST anomalies in the tropical Pacific between 12.5°N and 12.5°S, which represent 64, 70, 63, 41, and 58% of the variance in BCM, CERFACS, Hadley, INGV, and MPI, respectively, 46% in COADS, and 78% in NCEP (the smaller percentage in COADS results from the large amount of noise and gaps in the raw tropical Pacific data). Seasonally varying regression coefficients were then determined by least squares fit for each variable and grid point, using successive sets of three months to get smoothly varying estimates. The March regression was estimated from each February, March, and April (FMA), the April one from each March, April, and May (MAM),... The amount of removed variance varies somewhat between models but generally compares well with that removed from COADS or NCEP: Mostly less than 10% for the heat flux and 15% for SST, except in the Pacific where it can locally reach about 30% for SST. In the tropical Indian ocean, the ENSO signal in SST was substantially larger, which led us to exclude it from the analysis.

It should be noted that the method removes the instantaneous (on monthly time scale) linear effect of ENSO on Q' but not its possible delayed influence. However, Klein et al. (*1999*) have shown that the heat flux anomalies in the tropical North Atlantic and the South China Sea were best correlated with the simultaneous value of their ENSO index. It can thus be assumed that most of the (linear) ENSO influence on the surface heat flux is removed by our procedure. That the corresponding SST response to ENSO peaks after four to five months is irrelevant, since Eq. (3) is based on the relation between heat flux and prior SST anomalies.

The analysis procedure is the same for each model and the two reference data sets. However, to reduce the contamination by measurement errors, mesoscale eddies, interpolation, and sampling uncertainties, the anomaly fields in COADS were filtered by empirical orthogonal function (EOF) analysis in each ocean basin separately, reconstructing the fields from the first EOFs that accounted for 90% of their variance.

4 Global distribution of the heat flux feedback

4.1 Annual means

Figure 1 shows the net (turbulent plus radiative) heat flux feedback distribution for each model and the two "observed" data sets. Models with similar atmospheric (BCM and CERFACS) or oceanic (CERFACS and INGV) component are represented consecutively, while MPI follows INGV to stress the differences between ECHAM4 (INGV) and ECHAM5 (MPI). Overall, the net heat flux feedback is nearly everywhere negative. At extra-tropical latitudes, its geographical dependence is rather similar in the coupled models to that found in COADS and NCEP. However, the strength of the negative feedback is model dependent, with the largest values in INGV and the lowest ones in MPI. In both hemispheres, the heat flux feedback is strongly negative at mid latitudes between about 20 and 40° of latitude, generally ranging between 15 and 40 W m^{-2} K^{-1}, with largest values in the storm tracks on the western half of the ocean basins and in a narrow band tilting slightly northeastward in the North Pacific. In the North Atlantic, the negative feedback tends to be underestimated in the storm

track in all models but INGV, and the negative feedback maximum around 50°N seen in NCEP and, to a lesser extent, COADS is not reproduced, except in MPI where there is a weak maximum. Most models show a weakening of the negative feedback in the northern North Atlantic, but none of them reproduces the patches of positive feedback seen in NCEP north of about 60°N (note that the present analysis goes further north than in FK), or the corresponding tendency toward positive feedback seen at the northernmost COADS grid points (65°N). However, this area is much more under the influence of ice in several models. In the central North Pacific, the strong observed negative feedback is underestimated in the models, although to a lesser extent in CERFACS and INGV. The general underestimation of the negative feedback at northern mid latitudes could in part be linked to the limited resolution (T42 or equivalent) of the atmospheric models. Note that the feedback in the Atlantic in INGV is comparable to that found in a lower resolution version (T30) of the model (Frankignoul et al. *2002*), so that this possible influence may only come into play above a certain atmospheric resolution.

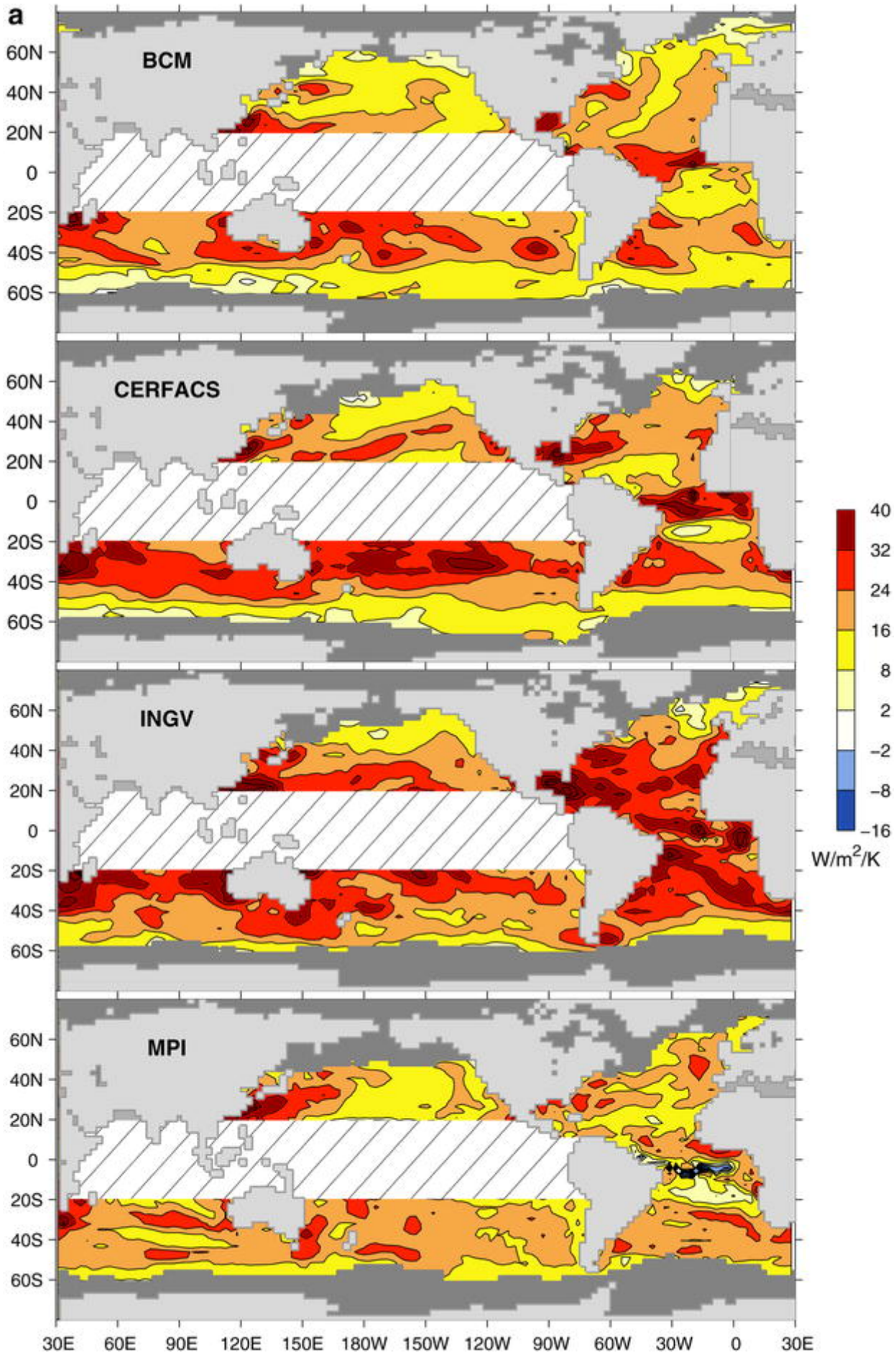
a
BCM
CERFACS
INGV
MPI
60N
40N
20N
0
20S
40S
60S
30E
60E
90E
120E
150E
180W
150W
120W
90W
60W
30W
0
30E
40
32
24
16
8
2
−2
−8
−16
W/m2/K

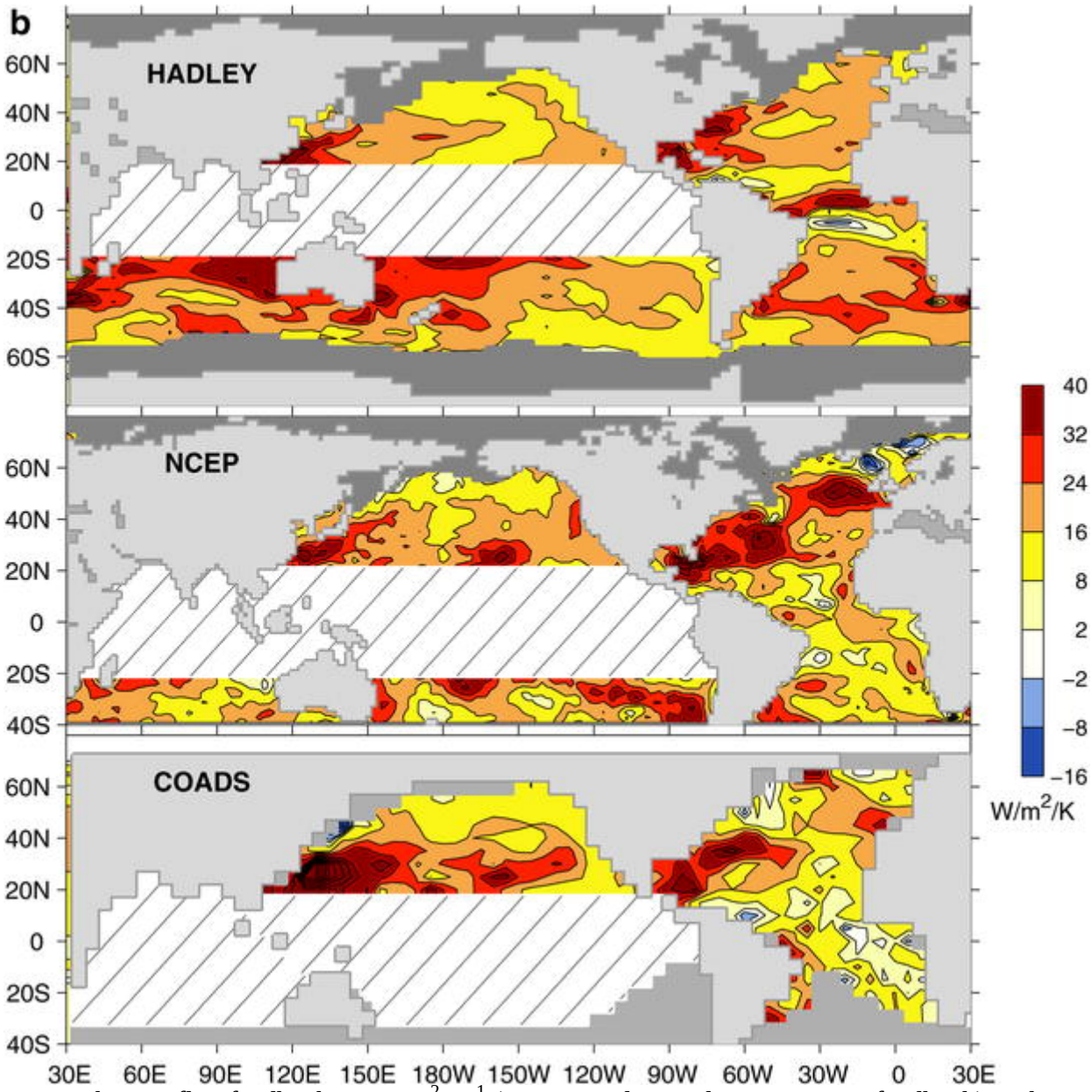

Fig. 1a, b Heat flux feedback in W m^{-2} K^{-1} (positive values indicate negative feedback) in the five coupled models, NCEP, and COADS. Areas where the monthly sea-ice coverage exceeds 20% during at least one year have been *blackened* (except in COADS where the *gray areas* indicate insufficient data coverage)

On the other hand, between 20 and 40°S, the negative feedback in the western and central South Pacific and in the Indian oceans tends to be stronger than in NCEP in all models but MPI. In the eastern South Pacific, a band of strong negative feedback is found in NCEP, and it is generally well reproduced, except in Hadley and MPI. We found no obvious link between these features and the surface wind climatologies.

The largest differences occur in the tropical Atlantic, where there is only little (positive or negative) feedback in COADS and a moderate negative feedback in NCEP. Instead, in all models but MPI, there is a band of large negative feedback broadly centered on the mean position of the Intertropical Convergence Zone (ITCZ). This negative feedback is very strong in CERFACS and INGV, with peaks exceeding 40 W m^{-2} K^{-1}, but more moderate in BCM and Hadley. As recalled in Sect. 3, the heat flux feedback estimates in the tropical Atlantic

may be slightly biased toward positive feedback, so that the feedback may even be more negative than in Fig. 1.

A more synthetic view of the feedback strength is given for the Atlantic in Fig. 2 by considering anomalies averaged across the basin in 10° latitudinal bands (5° at the equator). Note that the bands do not exactly correspond between all data sets, due to differences in grid sizes and sea-ice cover. As discussed in FK, the turbulent heat flux feedback is less negative at large spatial scales because of the scale dependence of the atmospheric response to diabatic heating (e.g., Frankignoul *1985*) and the efficiency of advection at removing heating perturbations in the boundary layer (e.g., Kleeman and Power *1995*). Hence, the large-scale feedback in Fig. 2 is typically smaller at extra-tropical latitudes than the average of the feedback in Fig. 1 over corresponding domains. At mid latitudes, the large-scale negative feedback in the North Atlantic ranges between 10 and 15 W m^{-2} K^{-1} in all coupled models, except in INGV where it is larger, but still smaller than in COADS and NCEP where the large-scale negative feedback exceeds 20 W m^{-2} K^{-1}. North of 40 or 50°N, the negative feedback is weaker in most data set, of the order of 10 W m^{-2} K^{-1}. In the northernmost band, CERFACS and INGV show a further weakening of the negative feedback, but none of the models has the reversal to positive feedback seen in NCEP. Note however that this domain is small and model-dependent, because of differences in sea-ice extent and grid size.

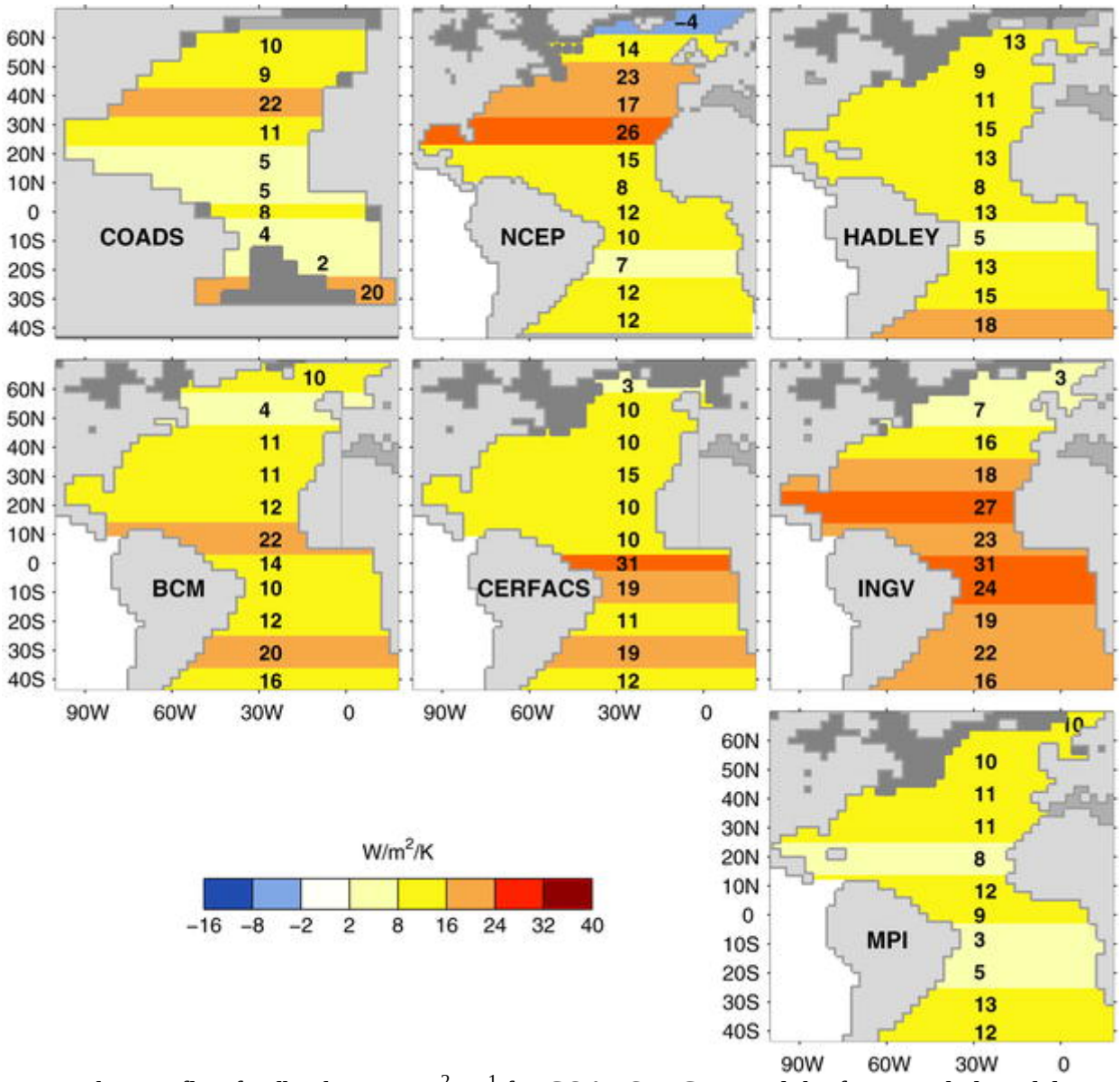

Fig. 2a, b Heat flux feedback in W m^{-2} K^{-1} for COADS, NCEP, and the five coupled models for Atlantic anomalies in 10° latitudinal bands (5° at the equator). *Positive* values indicate negative feedback. Areas where the monthly sea-ice coverage can exceed 20% during at least one year have been *blackened* (except in COADS where the *gray areas* indicate insufficient data coverage)

In the tropical Atlantic, the large-scale negative feedback increases from weakly negative in COADS, moderately negative in MPI, Hadley, NCEP, to strongly negative in BCM, CERFACS and INGV, reflecting the large discrepancies in Fig. 1. The negative feedback tends to be stronger along and near the equator, but it also ranges widely from a minimum of about 8 W m^{-2} K^{-1} in COADS and MPI to a maximum of 31 W m^{-2} K^{-1} in CERFACS and INGV, with BCM and Hadley in-between. In the south subtropical Atlantic, the large-scale heat flux feedbacks are generally comparable, ranging between 12 and 22 W m^{-2} K^{-1}.

Since BCM and CERFACS have a very similar atmospheric component (ARPEGE), and CERFACS and INGV an identical oceanic one (OPA), Figs. 1 and 2 suggest that both

components of the coupled models must influence the heat flux feedback in the tropics, mostly via the SST and the location of the ITCZ, as suggested later. At extra-tropical latitudes, the greater similarity between BCM and CERFACS than between CERFACS and INGV suggests that the feedback is primarily controlled by the atmosphere.

As in the observations, the net heat flux feedback in the coupled models is mostly due to the turbulent fluxes, except in the tropics where the surface radiative feedback also substantially contributes. In warm convective regions, a negative radiative feedback is expected from the direct atmospheric response to SST changes, warmer SST favoring deep convection and leading to more cirrus clouds in the upper troposphere, hence less incoming solar radiation (Ramanathan and Collins *1991*). On the other hand, the radiative feedback should be positive in regions with strong stratus coverage, because marine stratiform cloudiness is enhanced by lower SST, thereby decreasing surface insolation (Norris et al. *1998*). Note however that clouds of different height and optical thickness may respond differently to the SST changes, so that their net impact on the surface radiation may be quite complicated (e.g., Williams et al. *2003*). As shown in Fig. 3, the radiative feedback is always small at extra-tropical latitudes, with a tendency to be positive in the central and eastern subtropics, but negative in the western subtropics, consistent with the observed amount of low stratiform clouds (Klein and Hartmann *1993*). In the tropical Atlantic, the radiative feedback is weak in COADS (slightly negative in the west and positive in the east), and everywhere negative in NCEP, in particular along the equator in the west where it exceeds 10 W m^{-2} K^{-1}. The coupled models again show different behaviors: in BCM and Hadley, the radiative feedback is weakly negative in the western equatorial Atlantic, while it can have either sign further east, consistent with the observations. In CERFACS, it is everywhere negative but peaks in the Gulf of Guinea, exceeding 20 W m^{-2} K^{-1}. The same pattern is seen in INGV, but with values exceeding 30 W m^{-2} K^{-1}. In MPI the radiative feedback tends to be negative in the east but positive in the west and along the equator, presumably because the mean zonal SST gradient is inverted and the SST is minimum over South America (see Fig. 5 and 6 later). A synthetic view of the radiative feedback is given for zonal bands in the Atlantic in Fig. 4. At large scales, the radiative feedback remains small outside the tropics, but in the tropical Atlantic it ranges from very small in Hadley, MPI, COADS, and even NCEP to weakly negative in BCM, and strongly negative in CERFACS and INGV. It is shown later that these differences in radiative feedback are linked to the SST and, presumably, the cloud distribution.

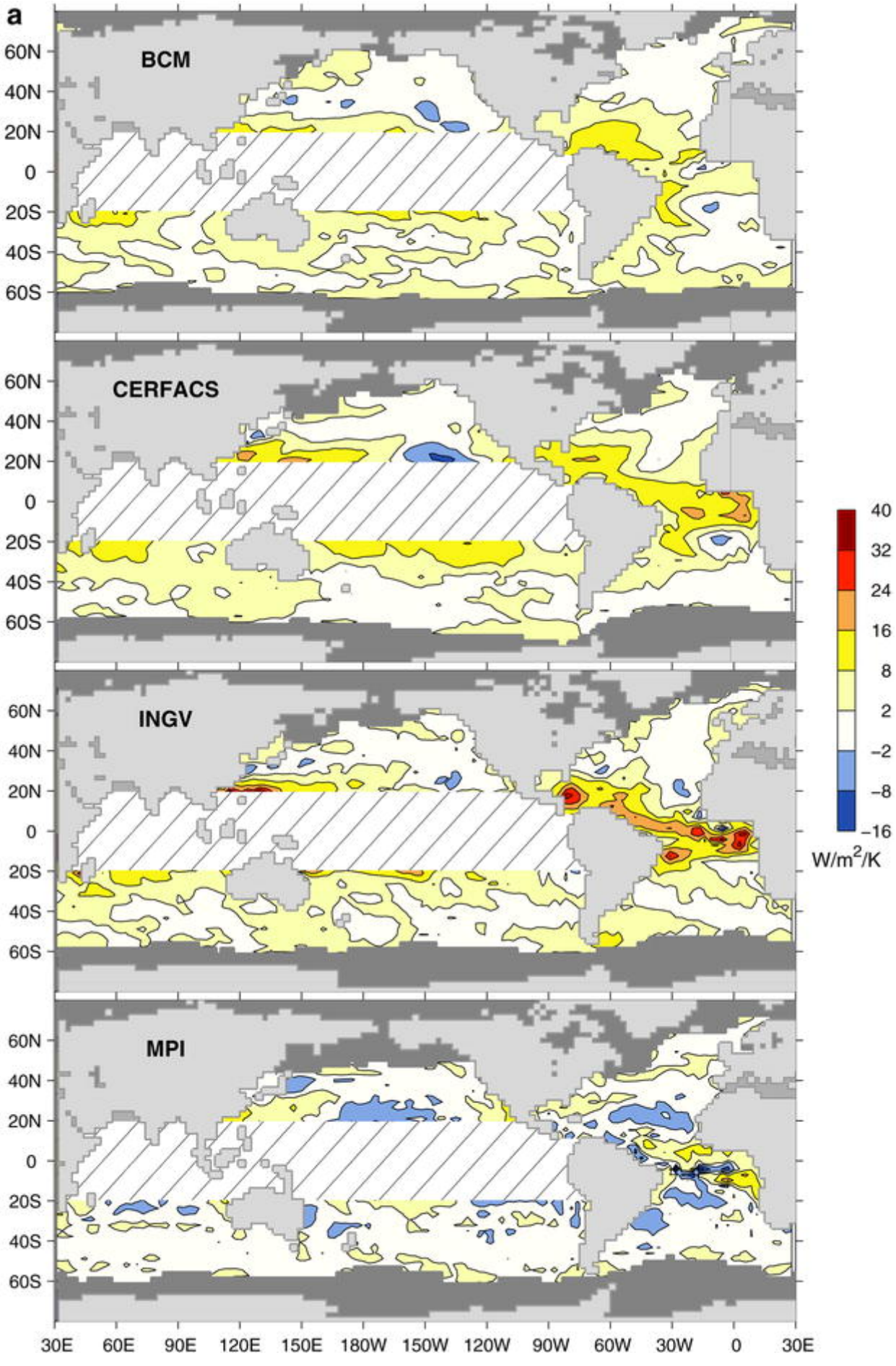
a
BCM
CERFACS
INGV
MPI
60N
40N
20N
0
20S
40S
60S
30E
60E
90E
120E
150E
180W
150W
120W
90W
60W
30W
0
30E
40
32
24
16
8
2
−2
−8
−16
W/m²/K

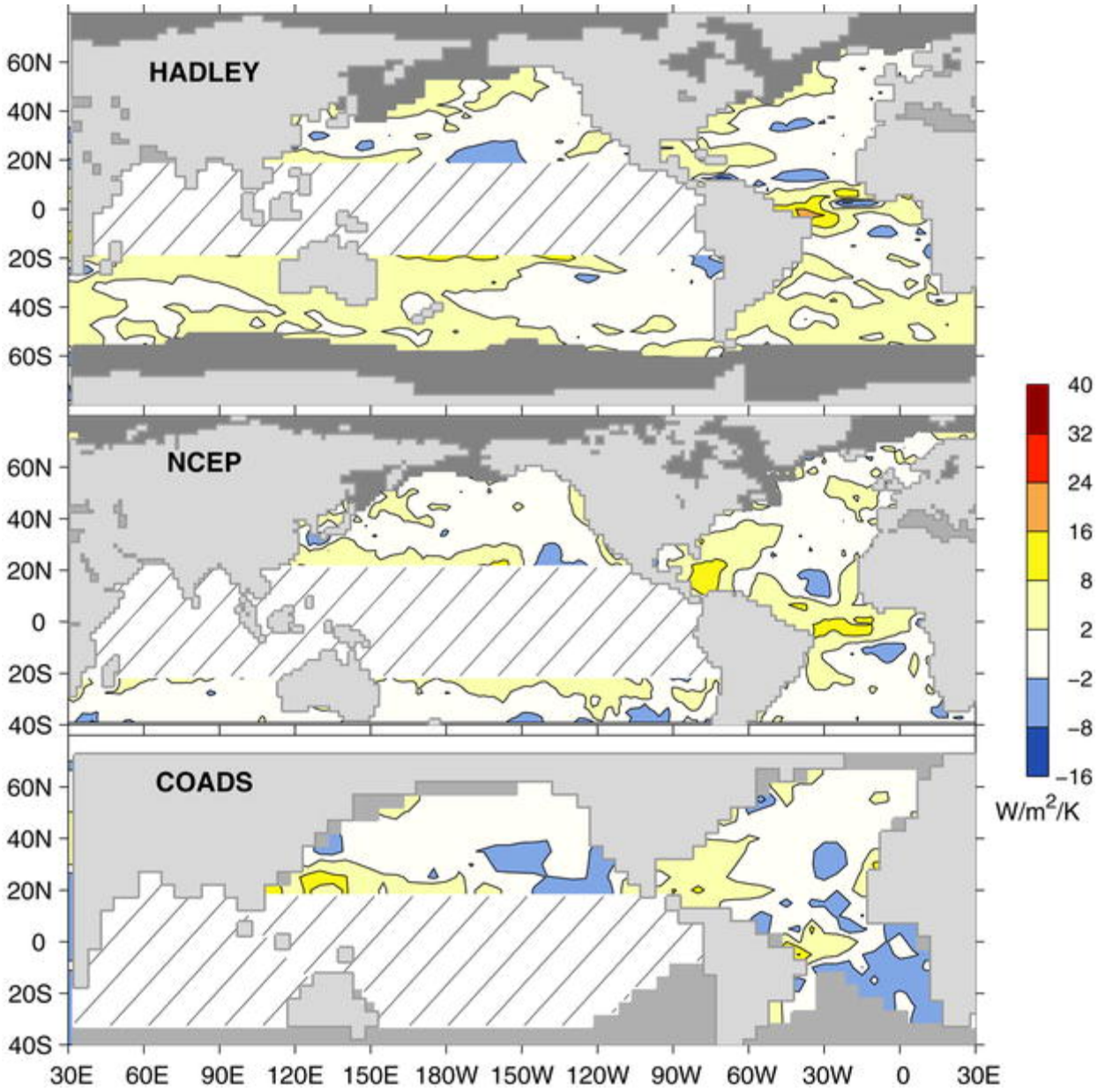

Fig. 3a, b As in Fig. 1 but for the radiative heat flux feedback

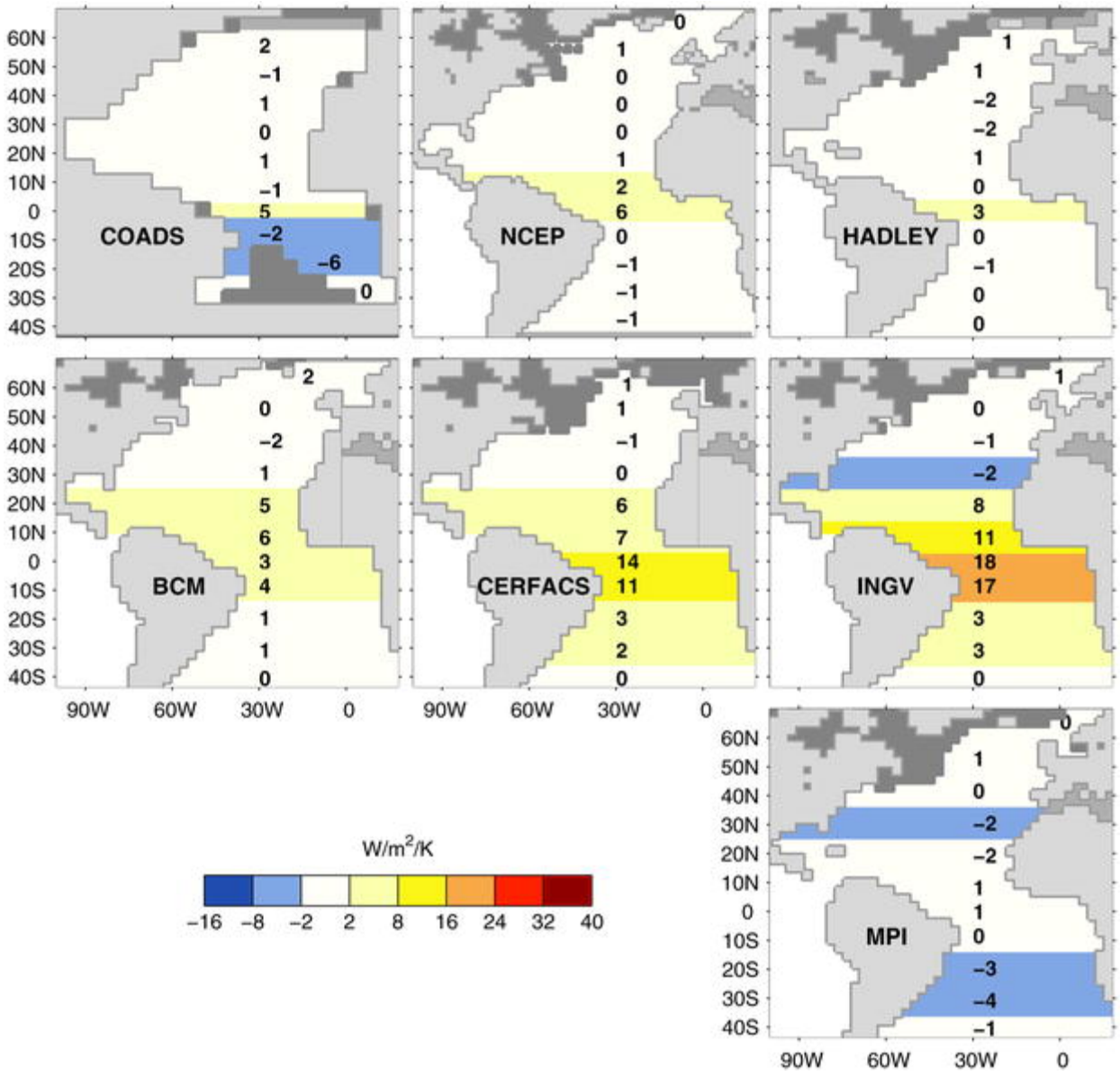

Fig. 4a, b As in Fig. 2 but for the radiative heat flux feedback

4.2 Seasonal variations

The seasonal cycle of the heat flux feedback in COADS and NCEP has been discussed in FK and, outside the tropical Atlantic, it is similar in the models. The turbulent heat flux feedback (and thus the net one) is more negative in the winter hemisphere and less negative in the summer one, consistent with the wind dependence of the bulk formulae for the turbulent fluxes. It is worth noting that the weak positive heat flux feedback seen in NCEP in the northern North Atlantic (Figs. 1 and 2) primarily comes from the turbulent heat flux feedback in winter and spring, and that only CERFACS has similar seasonal variations (not shown). At mid latitudes, the radiative feedback tends to be weakly positive in the summer hemisphere, consistent with observations in the North Pacific (Norris et al. *1998*), and weakly negative (less positive for MPI) in the winter one (see FK).

The seasonal variations of the heat flux feedback in the tropical Atlantic should be discussed, however, as they strongly differ between data sets. The position of the ITCZ and the SST maximum varies seasonally, being furthest south between February and April and north in August-September (Hastenrath *1991*). Most coupled models have difficulty in reproducing these seasonal variations, and indeed the ITCZ lies too far north in BCM, INGV, and MPI, and too far south in CERFACS and MPI, while the seasonal migration is realistic in Hadley. Some features of the SST climatology are illustrated in Figs. 5 and 6 (contours) for the two seasons that have the most contrasting heat flux feedback, focusing on the 15°S–15°N domain. Spring is defined by FMAM for SST and MAMJ for the heat flux, and summer by MJJA for SST and JJAS for the heat flux. As shown by the mean position of the 26, 27, and 28 °C isotherms contours (the other ones are not represented) in COADS and NCEP, spring corresponds to a southerly position of the ITCZ and summer to a northerly one.

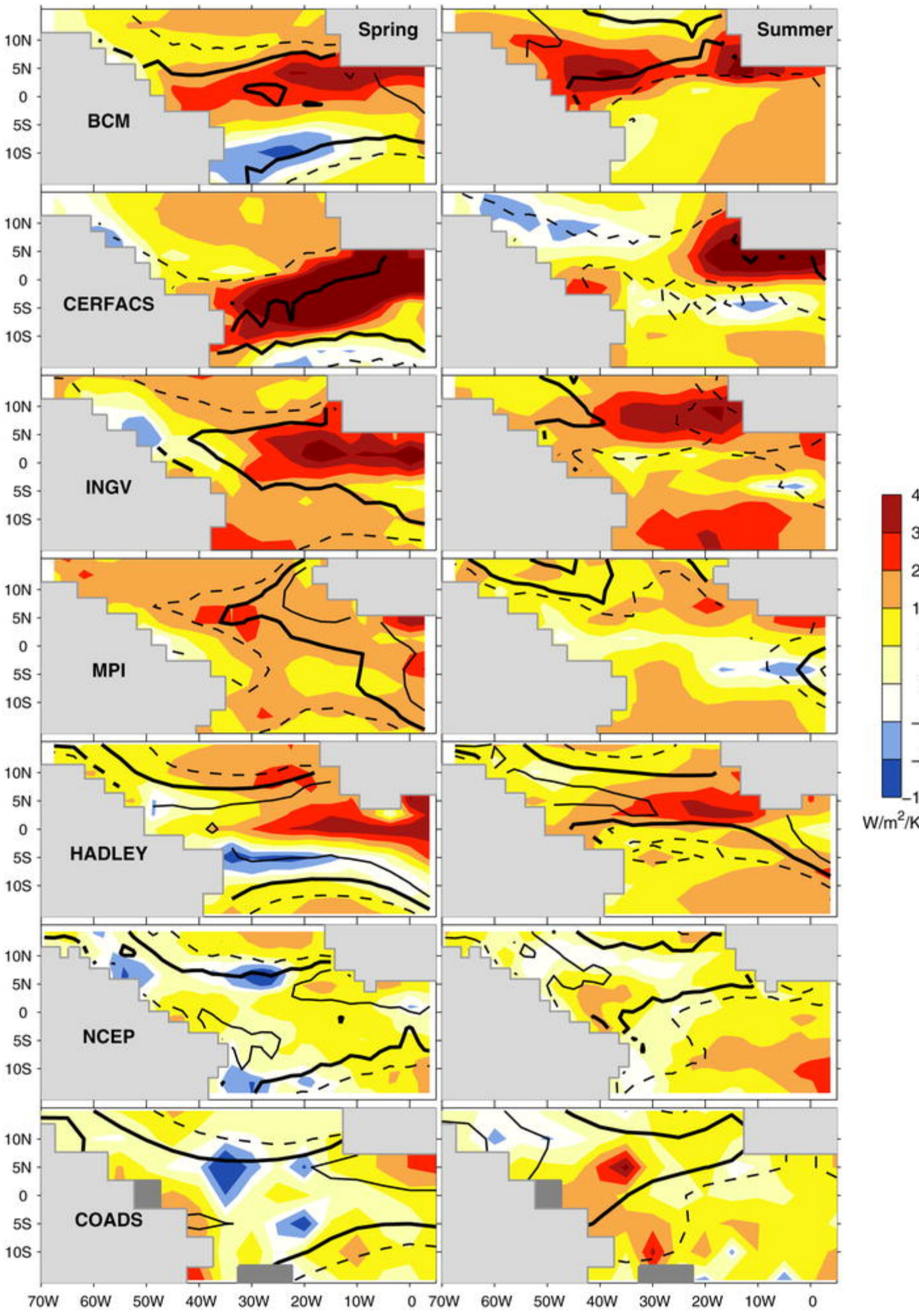
Spring
Summer
BCM
CERFACS
INGV
MPI
HADLEY
NCEP
COADS
10N
5N
0
5S
10S
70W
60W
50W
40W
30W
20W
10W
0
4
3
2
1
−1
W/m²/K

Fig. 5 Turbulent heat flux feedback in the tropical Atlantic (color scale, in W m^{-2} K^{-1}) and mean position of the 26 °C (*dashed line*), 27 °C (*heavy continuous line*), and 28 °C (*thin continuous line*) in spring (*left*) and summer (*right*) in the five coupled models, NCEP and COADS. *Positive values* indicate negative feedback

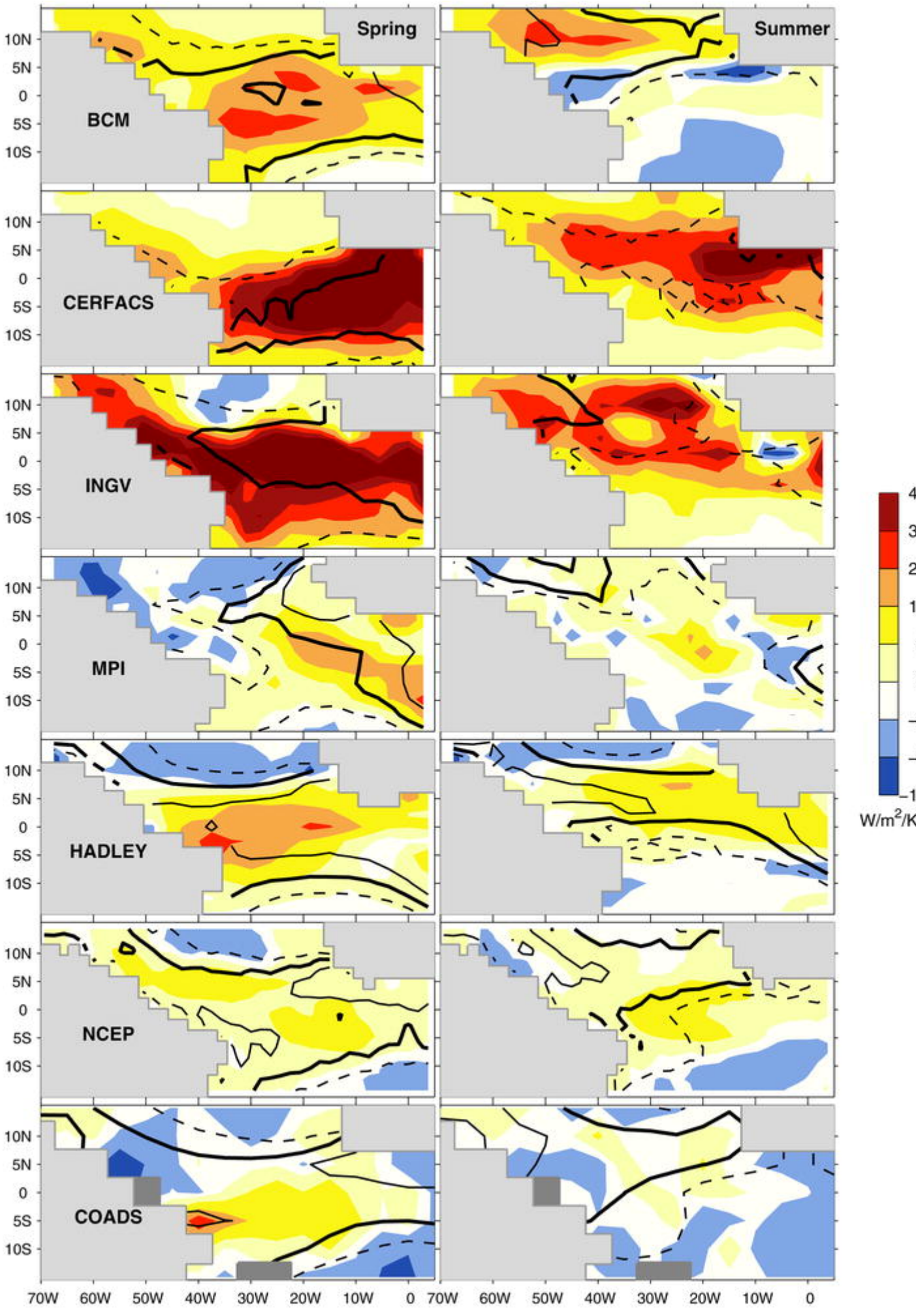
Spring
Summer
BCM
CERFACS
INGV
MPI
HADLEY
NCEP
COADS
10N
5N
0
5S
10S
70W
60W
50W
40W
30W
20W
10W
0
W/m²/K

Fig. 6 As in Fig. 5 but for the radiative heat flux feedback

As noted before, in all models the SST is much too warm in the southeastern Atlantic (less in BCM because of the heat flux correction), even though it is not striking in Figs. 5 and 6 because the colder isotherms are not shown. In spring, the SST climatology is otherwise rather realistic (differences less than 1 °C) in BCM, Hadley, except that it is too warm in the west, and INGV, except that it is too cold in the east and the Gulf of Guinea. The largest discrepancies with the observations are found in CERFACS, which is generally too cold (by up to 2 °C near the equator), and MPI, which is much too cold in the west and too warm in the east, so that SST increases eastward. In summer, the model-observations differences tend to be larger. BCM is too cold near the equator, except in the Gulf of Guinea, while Hadley is realistic, except in the Gulf of Guinea where it is too warm. The other models are too cold in the west and in the northeastern part of the domain, and too warm in the Gulf of Guinea.

The turbulent heat flux feedback is shown in Fig. 5 (color). Although the feedback estimated from Eq. (3) is less reliable since it is derived from a more limited sample and based on lag –1 only, COADS and NCEP are mostly in reasonable agreement, showing a stronger negative feedback (but still weak) in summer (right) than in spring (left), when there are more patches of positive feedback in both data sets, albeit at different locations. By contrast, in the coupled models the turbulent heat flux feedback tends to be more negative in spring than in summer. In spring (Fig. 5, left), the negative turbulent heat flux feedback is large in all the models but MPI, reaching 25 W m^{-2} K^{-1} over a substantial area of warm SST, with values exceeding 40 W m^{-2} K^{-1} along and to the north of the ITCZ in CERFACS, and along the equator in the Gulf of Guinea in INGV. BCM and Hadley have both an elongated patch of positive feedback in the west, south of the equator, with some limited correspondence with the (noisy) estimates in COADS or NCEP. In summer (Fig. 5, right), the turbulent heat flux feedback is too strong north of the equator in all models but MPI, in particular in BCM, CERFACS, and INGV. Note however that there is a band of weak positive feedback in CERFACS along 10°N that corresponds well to a band of negligible feedback in COADS and NCEP, but is not found in the other models. For brevity, the estimates in other seasons are not shown, but the agreement with COADS and NCEP remains limited in fall (except for INGV) and winter (except for Hadley).

The radiative feedback is shown for the same two seasons in Fig. 6. Again, although the estimates are noisy, there is some agreement between the main features in COADS and NCEP, with broad domains where the radiative feedback is either weakly positive or weakly negative. However, in spring COADS has areas with more substantial negative (near 5°S) or positive (near 5°N) feedback along the South American coast than NCEP. Except for the latter, a positive radiative feedback is mainly found where the mean SST is less than about 26 °C (dashed contour), presumably because the low-level static stability of the atmosphere is large and clouds are confined to the boundary layer. In spring, the feedback is only substantially negative when the SST exceeds 27 °C, but note that in NCEP (but not always in COADS) the negative feedback is weaker when the SST is above 28 °C, possibly because it is in the transition region between little and much convection that the SST anomalies have the largest impact. Whether this reflects reality or the representation of clouds in the NCEP model will not be speculated upon, but recall that the observations are sparse in these regions. In any case, in summer the correspondence is less clear, and the maximum negative feedback in NCEP is found in the central equatorial Atlantic over waters ranging between 26 and 27 °C.

In both seasons, the Hadley model has a rather realistic behavior, with mostly positive feedback above SST colder than about 26 °C, and negative feedback over warmer water. In BCM, there is a bias toward too strong negative feedback in spring and over warm northern waters in summer, but otherwise the geographic distribution of the radiative feedback is realistic. In both seasons, the most extreme behavior is found in CERFACS and INGV, with generally very strong negative feedback over SSTs larger than 26 °C, in particular in spring where it exceeds 40 W m^{-2} K^{-1} over large areas. In MPI, the radiative feedback in spring is positive (negative) over waters colder (warmer) than about 26 °C, as in the observations, but the geographic distribution of the feedback is not realistic because of the poor SST climatology. In summer the radiative feedback is generally small, not unlike that in NCEP. Again, fall and winter are not shown. In the observations as well as in the models, the radiative feedback in fall is similar to that in summer, and in winter it closely resembles the radiative feedback in spring, but often with weaker negative feedbacks.

It should be stressed that the discrepancies with the observations may not reflect an incorrect representation of the radiative impacts of clouds, but rather inadequacies in the cloud structure simulated by the models. The cloud response of the models should thus be evaluated, as in Williams at al. (2003), but this goes beyond the goals of the present study.

5 Influence on the persistence of SST anomalies

Since the heat flux feedback may substantially differ between models and the observations, in particular in the tropical Atlantic, it is of interest to determine whether it correspondingly leads to different SST anomaly time scale. FCL have suggested that the heat flux feedback contributes to about half the SST anomaly damping in the North Atlantic at mid latitudes away from large currents, where the simple stochastic climate model of Frankignoul and Hasselmann (*1977*) is applicable to a good approximation and the SST anomaly e-folding time set by the strength of the feedback processes. In the slab oceanic mixed layer model, the SST anomalies are well-represented by a first-order Markov process on time scales much longer than that of the atmospheric forcing, and their decay rate (or feedback factor λ) can be estimated from the SST anomaly autocovariance function $R_{TT}(\tau)$ that decays as $\exp(-\lambda\tau)$ for $\tau \gg 0$. As discussed in FCL and Frankignoul et al. (*2002*), the feedback factor can be decomposed into an oceanic contribution λ_o and an atmospheric one ($\lambda = \lambda_o + \lambda_a$), where the latter is related to the heat flux feedback α in Eq. (1) by

$$\lambda_o \approx \frac{\alpha}{\rho C_p \bar{h}} \qquad (6)$$

where $\rho C_p \bar{h}$ is the mean heat capacity of the oceanic surface mixed layer. If the heat flux feedback plays a significant role in determining the SST anomaly persistence, one expects α to be linearly related to λ_a. Hence, a coupled model with a stronger negative heat flux feedback should have shorter time scale SST anomalies, although some scatter is expected from the differences in mixed layer depth.

Although the heat flux feedback estimates remain valid in the presence of large mean currents, as pointed out by FK, their contribution to the SST anomaly decay rate is obscured at a fixed location by the effect of advection, which leads to an underestimation of the SST anomaly persistence (de Coëtlogon and Frankignoul *2003*). Also, in regions of substantial large-scale geostrophic variability as near the Gulf Stream, the SST anomaly time scale may

in addition be primarily set by the geostrophic fluctuations (e.g. Halliwell *1998*), not by feedback processes. Hence, we only investigate the relation between heat flux feedback and SST anomaly persistence south of the Gulf Stream and in large boxes by considering anomalies for latitudinal bands of 15° width, which reduces the influence of advection. As the model applies when the atmospheric forcing that generates the SST anomalies is essentially white at low frequencies, the SST anomaly persistence is estimated after (linear) removal of the ENSO signal, as in Sect. 3. The equatorial region is not considered since ocean dynamics have a strong influence on the SST anomalies and a stochastically forced slab model would be a poor approximation.

The parameter λ has been estimated from monthly SST anomalies, using FCL relation (A3) that takes into account the use of monthly averages, and the nonlinear fitting procedure of Levenberg and Marquardt (*1994*) at lag $\leq$ 3 months. To treat the models in the same way as COADS and NCEP, and to document the uncertainty of the calculation, the first and last 45 years of each simulation were considered separately, a third order polynomial estimated by least squares fit being removed from each anomaly time series.

A scatter plot of the estimated persistence versus the negative heat flux feedback is given for three domains in Fig. 7. Each model is represented by two dots that correspond to the two 45-year segments. There is a marked tendency for these independent estimates to cluster by model, suggesting the reliability of our calculation, with an accuracy of about 5 W m^{-2} K^{-1} for α and 0.1 $month^{-1}$ for λ. However, the SST anomaly persistence is smaller in COADS than NCEP, although they nearly correspond to the same time period. This is primarily due to the limited filtering applied to the COADS data (Sect. 2) that are more affected by irregular sampling, small-scale fluctuations, and data noise than the smoothed SSTs used in NCEP. The contamination should be larger in the tropics, where ship reports are sparse, leading to an underestimation of the SST persistence in COADS (an overestimation of λ). No bias is expected for the heat flux feedback, however, as the heat fluxes in COADS are calculated from the same individual ship observations as the SST.

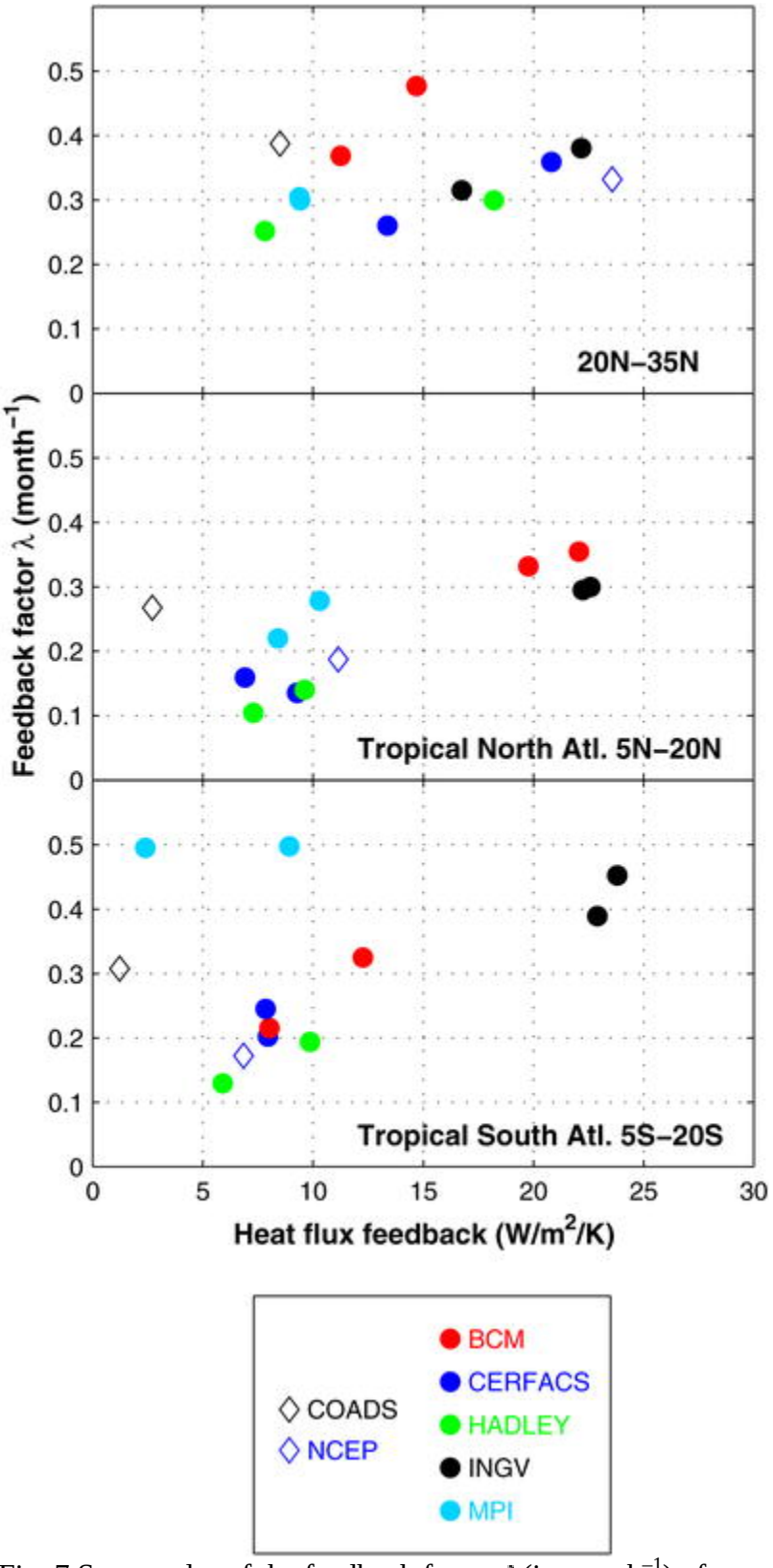

Fig. 7 Scatter plot of the feedback factor λ (in month^{-1}) of monthly SST anomalies versus heat flux feedback (in W m^{-2} K^{-1}) in COADS, NCEP and the five coupled models in three latitudinal domains. For each model, the estimates for the first and last 45 years are plotted

In the subtropical North Atlantic (Fig. 7, top), there is much scatter and only a hint of an increase in λ with the strength of the negative feedback, presumably because other processes such as subduction also play a role in controlling the SST anomaly persistence (de Coëtlogon and Frankignoul *2003*). In the tropical Atlantic, however, there is a general increase of the inverse SST anomaly persistence with increasing negative heat flux feedback both north and south of the equator, except that the SST damping in the South Atlantic is stronger in MPI than in the other models. Note that NCEP is consistent with the linear dependency suggested by the coupled models, and that the weaker COADS feedback would also roughly be if the SST anomaly persistence had been taken from NCEP.

In the two tropical Atlantic boxes, the approximate alignment of the points in Fig. 7 can be extrapolated to zero heat flux feedback, yielding $\lambda \approx 0.1$. Using this value as representative of the oceanic contribution to the SST anomaly damping, an admittedly crude step, suggests that the heat flux feedback λ_a might generally account for about half of the damping of the observed SST anomalies, but up to 3/4 in coupled models like INGV or BCM. This should explain why the atmospherically driven SST anomalies are too short-lived in these models.

6 Discussion and conclusions

At extra-tropical latitudes, the general features of the surface heat flux feedback are similar in the coupled models and the observed data sets. In particular, the net heat flux feedback is dominated by the turbulent fluxes, is nearly everywhere negative on an annual basis, and is strongest around the mid-latitude storm tracks. In North Atlantic, the negative feedback exceeds 40 W m^{-2} K^{-1} over substantial areas in COADS and NCEP (20 W m^{-2} K^{-1} for 10° latitudinal bands), but all models but INGV underestimate this maximum, sometimes by a factor of two. Comparing models with a very similar atmospheric (BCM and CERFACS) or oceanic (CERFACS and INGV) component suggests that the heat flux feedback differences between the coupled models primarily arise at mid latitudes from their atmospheric component. In the northern North Atlantic, the negative heat flux feedback strongly decreases in the observations and even becomes slightly positive at the northern edge, primarily because of the turbulent fluxes in winter and spring. This feature, which should enhance the SST variability near deep water formation regions, is only hinted upon in CERFACS.

The largest differences were found in the tropical Atlantic, where the observed feedback is weak, while it ranges between rather realistic (albeit slightly too negative) in Hadley and much too negative in INGV and, along the equator, CERFACS, where it exceeds 30 W m^{-2} K^{-1} at large scales. This occurs in part because the radiative fluxes strongly contributes to the negative feedback, in particular during spring. In the tropics, the heat flux feedback difference between the coupled models seems to be strongly linked to their SST climatology, hence the oceanic component plays a role as well. For instance, an inverted zonal SST gradient along the equator explains why the heat flux feedback is not realistic in MPI, even though it has the correct order of magnitude. Linking these results with the simulated atmospheric boundary layer and cloud structure should provide important information that may ultimately lead to improved model parametrizations, but this will be attempted elsewhere.

When summarizing the heat flux feedback intercomparison between the five coupled models, it should be kept in mind that the performance of a model may differ at mid latitudes and in

the tropics, hence that the ranking of the models may depend on the particular focus. Because it has the most realistic behavior in the tropical Atlantic and compares reasonably well with the observations elsewhere, Hadley shows the best overall behavior. BCM and CERFACS also seem fairly realistic, except for a too strong negative heat flux feedback in the tropical Atlantic, while MPI underestimates the negative feedback at mid latitudes. In INGV, the negative feedback is much too strong in the Atlantic, but elsewhere it also behaves reasonably well. In any case, there are biases in all of the models and there is thus room for improvement.

The differences in the heat flux feedback were shown to have a substantial impact on the characteristic SST anomaly time scale in the tropical Atlantic, so that models with a too strong negative heat flux feedback like INGV and BCM have too short-lived SST anomalies. A crude estimation suggests that, outside the equatorial waveguide, the heat flux feedback approximately accounts for about half of the damping of the observed SST anomalies, but up to 3/4 in coupled models like INGV or BCM. Note that the influence of the heat flux feedback is hardly seen in the subtropical North Atlantic, presumably because other processes such as subduction play an important role (de Coëtlogon and Frankignoul *2003*), or near the equator where the SST changes are primarily set by ocean dynamics. It would be of interest to establish if the heat flux feedback behaves similarly in the tropical Indo-Pacific, but the ENSO influence and the air-sea coupling are too strong for the present estimation method to be applicable.

Since the atmospheric adjustment to SST changes takes place rapidly, estimates of the heat flux feedback based on monthly data should remain applicable to all time scales. Coupled models with too strong negative heat flux feedback should underestimate the amplitude of the atmospherically driven SST anomalies but exaggerate the influence of the SST anomalies on climate when the SST changes are of oceanic origin. Increasing evidence (e.g., Latif et al. 2003) suggests that, on centenial time scales, changes in the mean overturning circulation create substantial interhemispheric SST changes. Our analysis suggests that the latter should be damped by the negative heat flux feedback. Latif et al. (2003) found that the centennial SST in the MPI run were indeed damped by the surface heat exchanges. This is reproduced in Fig. 8 which compares the time evolution of the low-frequency anomalies in SST and net surface heat flux in the North Atlantic domain 40–60°N, 50–10°W in the 500-year MPI run (here the heat flux is positive upward to facilitate the comparison). Although there is some scatter, as expected from spatial non-homogeneity, the two fields have a similar behavior (correlation of 0.77) that is consistent with a negative heat flux feedback of about 10 W m^{-2} K^{-1}. Our estimate of the negative heat flux feedback from the monthly MPI data (years 72 to 202 of the 500-year run) is also 10 W m^{-2} K^{-1} for the same North Atlantic domain, which strongly confirms the relevance of the present calculation to climate variability on all time scales. Note that the corresponding feedback in COADS and NCEP is 8 and 22 W m^{-2} K^{-1}, respectively, in broad agreement with the MPI values if one recalls the high bias of the NCEP turbulent fluxes in the North Atlantic (Josey *2001*). That a model with a too weak or too strong heat flux feedback would underestimate or overestimate the impact of such SST anomalies stresses that a good representation of the heat flux feedback is required for a realistic simulation of the climate variability, whether natural or forced. It is fortunate that this can be easily established from relatively short model simulations.

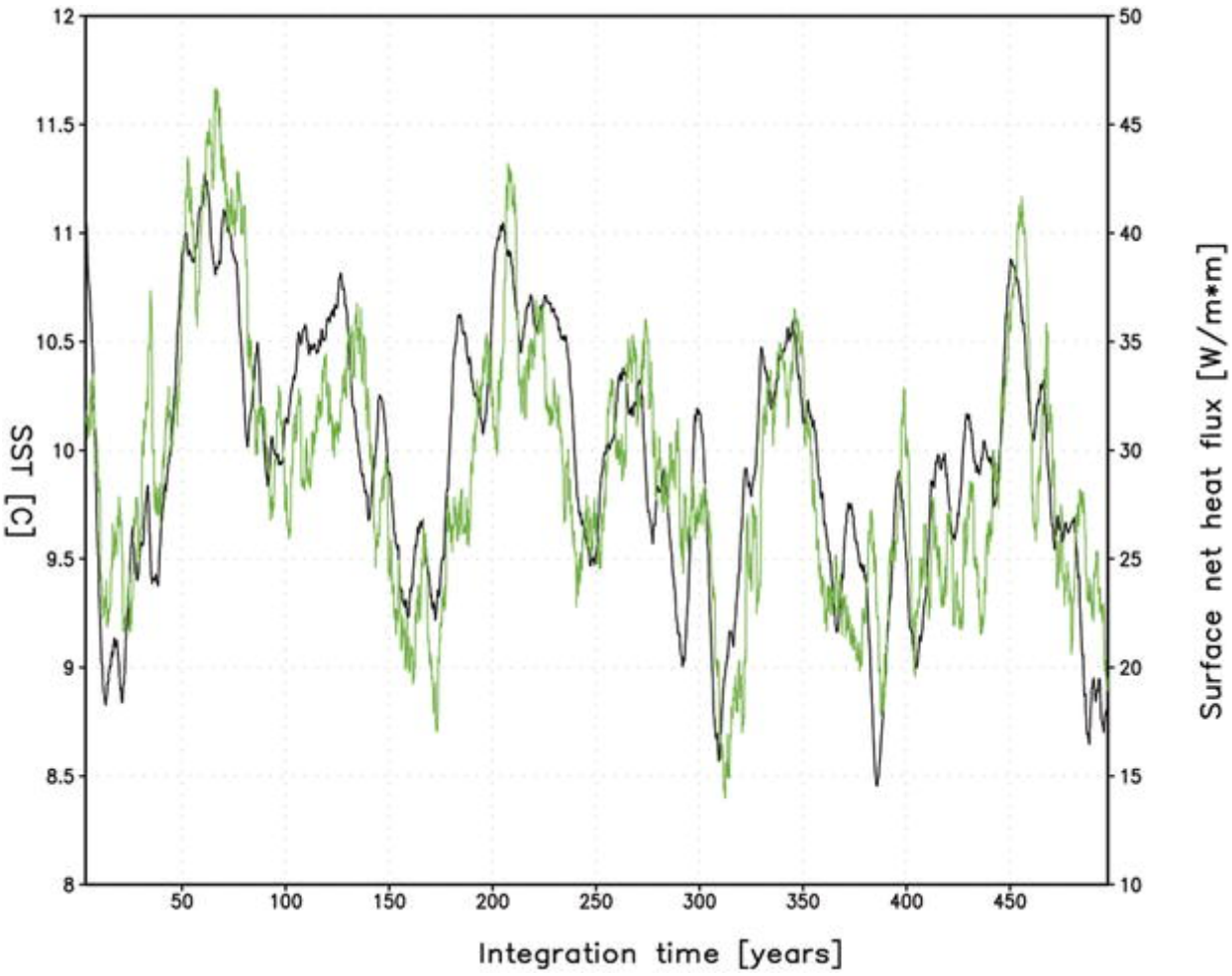

Fig. 8 Time behavior of the yearly anomalies in SST (*continuous*) and net surface heat flux (*positive upward*, *green*) in the 40–60°N, 50–10°W domain in the simulation with the MPI model. The data have been low-passed filtered using a 5-year running mean

Acknowledgements The NCAR/NCEP Reanalysis data was provided through the NOAA Climate Center (http://www.cdc.noaa.gov/), and COADS by Dan Cayan, Climate Research Division, Scripps Institution of Oceanography. This research was supported by the PREDICATE project of the European Community.

References

Barsugli JJ, Battisti DS (1998) The basic effects of atmosphere-ocean thermal coupling on midlatitude variability. J Atmos Sci 55: 477–493

Bleck R, Rooth C, Hu D, Smith LT (1992) Salinity-driven thermocline transients in a wind- and thermohaline-forced isopycnic coordinate model of the North Atlantic. J Phys Oceanogr 22: 1486–1505

Chang P, Ji L, Li H (1997) A decadal climate variation in the tropical Atlantic Ocean from thermodynamic air-sea interactions. Nature 385: 516–518

Chang P, Ji L, Saravanan R (2001) A hybrid coupled model study of tropical Atlantic variability. J Clim 14: 361–390

Czaja A, van der Vaart P, Marshall J (2002) A diagnostic study of the role of remote forcing in tropical Atlantic variability. J Clim 15: 3280–3290

Davey MK, Huddleston M, Sperber KR, Braconnot P, Bryan F, Chen D, Colman RA, Cooper C, Cubasch U, Delecluse P, DeWitt D, Fairhead L, Flato G, Gordon C, Hogan T, Ji M, Kimoto M, Kitoh A, Knutson TR, Latif M, Le Treut H, Li T, Manabe S, Mechoso CR, Meehl GA, Power SB, Roeckner E, Terray L, Vintzileos A, Voss R, Wang B, Washington WM, Yoshikawa I, Yu JY, Yukimoto S, Zebiak SE (2002) STOIC: a study of coupled model climatology and variability in tropical ocean regions. Clim Dyn 18: 403–420

de Coëtlogon G, Frankignoul C (2003) On the persistence of winter sea surface temperature in the North Atlantic. J Clim 16: 1364–1377

Déqué M, Dreveton C, Braun A, Cariolle D (1994) The ARPEGE/IFS atmosphere model: a contribution to the French community climate modelling. Clim Dyn 10: 249–266

Fichefet T, Morales Maqueda MA (1997) Sensitivity of a global sea ice model to the treatment of ice thermodynamics and dynamics. J Geophys Res 102: 12,609–12,646

Frankignoul C (1985) Sea surface temperature anomalies, planetary waves and air-sea feedback in the middle latitudes. Rev Geophys 23: 357–390

Frankignoul C, Hasselmann K (1977) Stochastic climate models. Part II. Application to sea-surface temperature variability and thermocline variability. Tellus 29: 284–305

Frankignoul C, Czaja A, L'Heveder B (1998) Air-sea feedback in the North Atlantic and surface boundary conditions for ocean models. J Clim 11: 2310–2324

Frankignoul C, Kestenare E, Sennéchael N, de Coëtlogon G, D'Andrea F (2000) On decadal-scale ocean-atmosphere interactions in the extended ECHAM1/LSG climate simulation. Clim Dyn 16: 333–354

Frankignoul C, Kestenare E (2002) The surface heat flux feedback. Part I: estimates from observations in the Atlantic and the North Pacific. Clim Dyn 19: 633–647

Frankignoul C, Kestenare E, Mignot J (2002) The surface heat flux feedback. Part II: direct and indirect estimates in the ECHAM4/OPA8 coupled GCM. Clim Dyn 19: 649–655

Furevik T, Bensen M, Drange H, Kindem IKT, Kvamstø NG, Sorteberg A (2003) Description and evaluation of the bergen climate model: ARPEGE coupled with MICOM. Clim Dyn 21:27–51

Gordon C, Cooper C, Senior CA, Banks H, Gregory JM, John TC, Mitchell JFB, Wood RA (2000) The simulation of SST, sea ice extents and ocean heat transports in a version of the Hadley Centre coupled model without flux adjustments. Clim Dyn 16: 147–168

Grötzner A, Latif M, Barnett TP (1998) A decadal climate cycle in the North Atlantic ocean as simulated by the ECHO coupled GCM. J Clim 11: 831–847

Gualdi S, Navarra A, Guilyardi E, Delecluse P (2003) Assessment of the tropical Indo-Pacific climate in the SINTEX CGCM. Ann Geophys 46: 1–26

Halliwell GR Jr (1998) Simulation of North Atlantic decadal/multidecadal winter SST anomalies driven by basin-scale atmospheric circulation anomalies. J Phys Oceanogr 28: 5–21

Hastenrath S (1991) Climate dynamics of the tropics. Kluwer Academic, Dordrecht, NL, pp 488

Hoerling MP, Kumar A, Zhong M (1997) El Niño, La Nina, and the nonlinearity of their teleconnections. J Clim 10: 1769–1786

Josey SA (2001) A comparison of ECMWF, NCEP-NCAR, and SOC surface heat fluxes with moored buoy measurements in the subduction region of the Northeast Atlantic. J Clim 14: 1780–1789

Jouzeau A, Maisonnave E, Valcke S, Terray L (2003) Climatology and interannual to decadal variability diagnosed from a 200-year global coupled experiment. CERFACS Techn Rep

Kalnay E and Coauthors (1996) The NCEP/NCAR Reanalysis Project. Bull Am Meteorol Soc 77: 437–471

Klein SA, Hartmann DL (1993) The seasonal cycle of low stratiform clouds. J Clim 6: 1587–1606

Klein SA, Soden BJ, Lau N-C (1999) Remote sea surface temperature variations during ENSO: Evidence for a tropical atmospheric bridge. J Clim 12: 917–932

Kleeman R, Power SB (1995) A simple atmospheric model of surface heat flux for use in ocean modeling studies. J Phys Oceanogr 25: 92–105

Latif M, Barnett TP (1994) Causes of decadal climate variability in the North Pacific/North American sector. Science 266: 634–637

Levenberg, Marquardt (1994) The art of scientific computing, 2nd edn. Cambridge University Press, Cambridge, UK, pp 994

Madec G, Delecluse P, Imbard M, Levy C (1998) OPA 8.1 ocean general circulation model reference manual, Internal Rep 11. Institut Pierre-Simon Laplace (IPSL), France, pp 91

Marsland SJ, Haak H, Jungclaus JH, Latif M, Roeske F (2003) The Max-Planck-Institute global ocean/sea ice model with orthogonal curvilinear coordinates. Ocean Modell 5: 91–127

Norris JR, Zhang Y, Wallace JM (1998) Role of low clouds in summertime atmosphere-ocean interactions over the North Pacific. J Clim 11: 2482–2490

Pope VD, Gallani ML, Rowntree PR, Stratton RA (2000) The impact of new physical parametrizations in the Hadley Centre climate model: HadAM3. Clim Dyn 16: 123–146

Ramanathan V, Collins W (1991) Thermodynamic regulation of ocean warming by cirrus clouds deduced from observations of the 1987 El Niño. Nature 13: 325–347

Roeckner E, Arpe K, Bengtsson L, Christoph M, Claussen M, Dümenil L, Esch M, Giorgetta M, Schlese U, Schulzweida U (1996) The atmospheric general circulation model ECHAM-4:

Model description and simulation of present-day climate. Max-Planck-Institute für Meteorologie, Rep. 218, pp 90

Roeckner E et al (2003) The atmospheric general circulation model ECHAM5: Part I: model description. MPI Report (Available from the Max-Planck-Institut fuer Meteorologie, Bundesstr. 55, 20146 Hamburg)

Sutton R, Mathieu PP (2002) Response of the atmosphere–ocean mixed layer system to anomalous ocean heat flux convergence. Q J R Meteorol Soc 128: 1259–1275

Trenberth KE, Caron JM, Stepaniak DP (2001) The atmospheric energy budget and implications for surface fluxes and ocean heat transports. Clim Dyn 17: 259–276

Von Storch JS (2000) Signature of air-sea interactins in a coupled atmosphere-ocean GCM. J Clim 13: 3361–3379

Williams KD, Ringer MA, Senior CA (2003) Evaluating the cloud response to climate change and current climate variability. Clim Dyn 20: 705–721

Xie SP, Philander SGH (1994) A coupled ocean–atmosphere model of relevance to the ITCZ in the eastern Pacific. Tellus 46A: 340–350

Zorita E, Frankignoul C (1997) Modes of North Atlantic decadal variability in the ECHAM1/LSG coupled ocean–atmosphere general circulation model. J Clim 10: 183–200